# Hydrogen-1, Carbon-13, and Nitrogen-15 NMR Spectroscopy of *Anabaena* 7120 Flavodoxin: Assignment of β-Sheet and Flavin Binding Site Resonances and Analysis of Protein–Flavin Interactions†

Brian J. Stockman,‡ Andrzej M. Krezel, and John L. Markley*

*Department of Biochemistry, College of Agricultural and Life Sciences, 420 Henry Mall, University of Wisconsin—Madison, Madison, Wisconsin 53706*

Karin G. Leonhardt and Neil A. Straus

*Department of Botany, University of Toronto, Toronto, Ontario M5S 1A1, Canada*

*Received May 9, 1990; Revised Manuscript Received July 10, 1990*

ABSTRACT: Sequence-specific $^1H$ and $^{13}C$ NMR assignments have been made for residues that form the five-stranded parallel β-sheet and the flavin mononucleotide (FMN) binding site of oxidized *Anabaena* 7120 flavodoxin. Interstrand nuclear Overhauser enhancements (NOEs) indicate that the β-sheet arrangement is similar to that observed in the crystal structure of the 70% homologous long-chain flavodoxin from *Anacystis nidulans* [Smith et al. (1983) *J. Mol. Biol. 165*, 737–755]. A total of 62 NOEs were identified: 8 between protons of bound FMN, 29 between protons of the protein in the flavin binding site, and 25 between protons of bound FMN and protons of the protein. These constraints were used to determine the localized solution structure of the FMN binding site. The electronic environment and conformation of the protein-bound flavin isoalloxazine ring were investigated by determining $^{13}C$ chemical shifts, one-bond $^{13}C$–$^{13}C$ and $^{15}N$–$^1H$ coupling constants, and three-bond $^{13}C$–$^1H$ coupling constants. The carbonyl edge of the flavin ring was found to be slightly polarized. The xylene ring was found to be nonplanar. Tyrosine 94, located adjacent to the flavin isoalloxazine ring, was shown to have a hindered aromatic ring flip rate.

Flavodoxins constitute a group of low molecular weight (14000–23000) FMN-containing[1] flavoproteins that mediate electron transfer at low redox potential between the prosthetic groups of other proteins (Mayhew & Ludwig, 1975). Flavodoxins have been shown to serve as replacements for ferredoxins (iron–sulfur proteins), in certain electron-transfer reactions (Tollin & Edmondson, 1980). In some organisms, the flavodoxin used in photosynthetic electron transport is produced constitutively, while in others it is produced only under conditions of limiting iron.

The flavin cofactor (FMN) has three oxidation states: oxidized, semiquinone (one-electron-reduced), and hydroquinone (two-electron-reduced). The redox potentials of both oxidized-semiquinone ($E_1$) and semiquinone-reduced ($E_2$) transitions in FMN are altered by its association with the apoprotein. In *Anabaena* 7120 flavodoxin, $E_1$ is −196 mV and $E_2$ is −425 mV (Paulsen et al., 1990), while those of free flavin are −238 and −172 mV, respectively (Simondson & Tollin, 1980). Similar protein-induced redox potential modulations have been reported for other flavoproteins (Simondson & Tollin, 1980: Sykes & Rogers, 1984). Alteration of the FMN redox potential by the protein enables nature to fine tune flavodoxins to function in specific reactions.

As part of a long-term goal to understand the structure-function interactions that underlie redox potential manipulation in *Anabaena* 7120 flavodoxin, we have used $^{13}C$- and $^{15}N$-enriched protein samples to assist in assigning $^1H$, $^{13}C$, and $^{15}N$ signals from bound FMN and from the amino acid residues in the consensus flavin binding site. In addition, resonances from amino acid residues forming the five-stranded parallel β-sheet core of the protein have been assigned. With these assignments in hand, $^{13}C$ spectral editing techniques were employed in NOE studies of the structure of the FMN binding site. $^{13}C$ chemical shifts and $^{13}C$–$^{13}C$, $^1H$–$^{13}C$, and $^{15}N$–$^1H$ coupling constants determined for the bound flavin cofactor have been used to characterize its conformation. These values provide information regarding the electronic environment and solvent accessibility of the flavin isoalloxazine ring and the local structure of the flavin binding site in solution. Protein–FMN interactions determined here by NMR are compared to those observed by X-ray crystallography (Smith et

† Supported by USDA Competitive Research Grant 88-37262-3406, NIH Grant RR02301, and the New Energy and Industrial Technology Development Organization (Tokyo, Japan). This study made use of the National Magnetic Resonance Facility at Madison, which is supported in part by NIH Grant RR02301 from the Biomedical Research Technology Program, Division of Research Resources. Equipment in the facility was purchased with funds from the University of Wisconsin, the NSF Biological Biomedical Research Technology Program (Grant DMB-8415048), the NIH Shared Instrumentation Program (Grant RR02781), and the U.S. Department of Agriculture. B.J.S. was supported by an NIH Training Grant in Cellular and Molecular Biology (GM07215).

* To whom correspondence should be addressed.

‡ Present address: Biophysics Research Division, University of Michigan.

[1] Abbreviations: COSY, correlated spectroscopy; DQC, double quantum correlation; DQF-COSY, double-quantum-filtered correlated spectroscopy; $E_1$, midpoint potential for the oxidized-semiquinone transition at pH 7.0; $E_2$, midpoint potential for the semiquinone-reduced transition at pH 7.0; FAD, flavin adenine dinucleotide; FMN, flavin mononucleotide; HOHAHA, homonuclear Hartmann–Hahn; INADEQUATE, incredible natural abundance double quantum transfer; MBC, multiple-bond correlation; NOE, nuclear Overhauser enhancement; NOESY, nuclear Overhauser enhancement spectroscopy; pH*, pH meter reading without correction for the deuterium isotope effect; RELAY, relayed correlated spectroscopy; ROE, rotating frame Overhauser enhancement; ROESY, rotating frame Overhauser enhancement spectroscopy; SBC, single-bond correlation; SBC-NOE, single-bond correlation with NOE relay; TARF, tetraacetylriboflavin; TMS, tetramethylsilane; TSP, (trimethylsilyl)propionic acid; U, uniformly labeled.

0006-2960/90/0429-9600$02.50/0 

```
                1        10        20        30        40
A. 7120      SKKIGLFYGTQ  TGKTESVAEI  IRDEFGND-V  VTLHDVSQAE
             ||||||||||  ||.|.''||.  |.|||.'.'  |.|.|.'.'.
A. nidulans  AKIGLFYGTQ  TGVTQTIAES  IQQEFGGESI  VDLNDIANAD

                    50        60        70        80
A. 7120      VTDLNDYQYL  IIGCPTWNIG  ELQSDWEGLY  SELDDVDFNG
             ''|||.|.||  ||||||||'.|  ||||||||'.|  '.||.|.'.|
A. nidulans  ASDLNAYDYL  IIGCPTWNVG  ELQSDWEGIY  DDLDSVNFQG

                    90        100       110       120
A. 7120      KLVAYFGTGD  QIGYADNFQD  AIGILEEKIS  QRGGKTVGYW
             |.|||||.||  |'.||.||||  |.||||||||  |.|||||
A. nidulans  KKVAYFGAGD  QVGYSDNFQD  AMGILEEKIS  SLGSQTVGYW

                    130       140       150       160
A. 7120      STDGYDFNDS  KALRNGKFVG  LALDEDNQSD  LTDDRIKSWV
             '.|||||'.|  ||'.||.|||  ||'.|||||.|  ||.|||'.||
A. nidulans  PIEGYDFNES  KAVRNNQFVG  LAIDEDNQPD  LTKNRIKTWV

                169
A. 7120      AQLKSEFGL
             |||||||||
A. nidulans  SQLKSEFGL
```

FIGURE 1: Comparison of primary sequences of *Anabaena* 7120 (Leonhardt & Straus, 1989) and *A. nidulans* (Laudenbach et al., 1987) flavodoxins. Consensus flavin binding site residues are in boldface. Strictly conserved residues are indicated by bars and conservative replacements by dots.

al., 1983; Laudenbach et al., 1987) in the 70% homologous flavodoxin from *Anacystis nidulans* (Leonhardt & Straus, 1989). The primary sequences of the two flavodoxins are compared in Figure 1.

## Materials and Methods

*Protein Enrichment and NMR Sample Preparation.* *Anabaena* 7120 was grown as described previously (Stockman et al., 1988a). To obtain protein uniformly enriched with $^{13}C$, $^{13}CO_2$ (26 atom % isotopic purity) was supplied to the growth medium as the sole carbon source. Protein uniformly enriched with $^{15}N$ was obtained by growing the cyanobacterium on $K^{15}NO_3$ as the sole nitrogen source. Flavodoxin was purified by the procedure of D. W. Krogmann and C. Harper (Harper, 1988). Protein fractions with $A_{466}/A_{276}$ ratio greater than 0.14 were considered to be pure. NMR samples were typically 5–8 mM protein in 0.45 mL of 100 mM phosphate buffer. The pH* was adjusted to 7.5. For spectra collected in $^2H_2O$, the protein was lyophilized and resuspended in $^2H_2O$ several times.

*Preparation of [26% U-$^{13}C$ FMN]Flavodoxin.* Unlabeled apoflavodoxin was prepared from 30 mg of unlabeled flavodoxin by dialysis vs 2 M KBr at pH 3.9 (Mayhew, 1971). [26% U-$^{13}C$]FMN was prepared by trichloroacetic acid precipitation of 30 mg of [26% U-$^{13}C$]flavodoxin. The complexation of FMN and apoflavodoxin was instantaneous upon their combination, as judged by a change in color from the characteristic bright yellow of FMN (maximum absorbance 445 nm) to the light orange of oxidized *Anabaena* 7120 flavodoxin (maximum absorbance 466 nm).

*Chemicals.* $^{13}CO_2$ (99+ atom %) was purchased from Isotec, Inc. The $^{13}CO_2$ was diluted with natural abundance $CO_2$ and mixed with air to 10% $CO_2$. The level of $^{13}C$ was about 26 atom % isotopic purity (as measured by $^{13}C$ satellite intensities in the $^1H$ NMR spectra of individual amino acids which showed this level of incorporation). $K^{15}NO_3$ (99+ atom %) was purchased from Isotec. Other chemicals were of reagent grade or better.

*NMR Spectroscopy.* All spectra were recorded at 298 ± 1 K on Bruker AM-500 (11.7 T) or Bruker AM-600 (14.2 T) spectrometers. Proton chemical shifts are referenced to internal TSP. Experimental carbon chemical shifts were determined relative to external dioxane, which was assigned a chemical shift of 67.8 ppm relative to TMS. Experimental nitrogen chemical shifts were determined relative to external ammonium sulfate, which was assigned a chemical shift of 22.3 ppm relative to liquid ammonia.

$^{13}C\{^{13}C\}$DQC spectra (125.77 MHz) were collected by using a Bruker 5-mm broad-band probe and a $^{13}C$-selective preamplifier. The pulse sequence used was a modification (Westler et al., 1988a) of the resonance-offset-compensated INADEQUATE experiment (Levitt & Ernst, 1983). WALTZ-16 (Shaka et al., 1983) composite pulse decoupling was used during acquisition to decouple attached protons.

$^1H\{^{13}C\}$SBC, $^1H\{^{13}C\}$SBC-NOESY, $^1H\{^{13}C\}$MBC, and $^{13}C$-edited $^1H\{^1H\}$NOESY spectra were collected in the Bruker reverse electronics mode with a Bruker 5-mm inverse broad-band probe. The decoupler was used for $^1H$ pulses, while the transmitter was used to pulse other nuclei. The pulse sequence used for the $^1H\{^{13}C\}$SBC experiments was that of Bax et al. (1983). The $^1H\{^{13}C\}$SBC-NOESY experiments used the method of Oh et al. (1989). WALTZ-16 decoupling at the carbon frequency was used during acquisition to collapse proton–carbon couplings. The pulse sequence for the $^1H\{^{13}C\}$MBC experiment was that of Bax and Summers (1986). In the $^{13}C$-edited $^1H\{^1H\}$NOESY experiment, $^{13}C$ was pulsed only to edit the spectrum and not during acquisition. This results in the proper cross-peak fine structure needed to extract $^3J_{CH}$ values (Montelione et al., 1989).

$^1H\{^1H\}$ data were collected with a standard Bruker proton probe. DQF-COSY (Rance et al., 1983) and NOESY (Anil Kumar et al., 1980; Bodenhausen et al., 1984) spectra were collected in the normal electronics mode with proton pulses supplied by the transmitter. The mixed NOESY–ROESY experiment (Fejzo et al., 1990) was carried out by using Bruker reverse electronics with proton pulses supplied by the decoupler. See the figure legends for additional experimental parameters.

*Molecular Modeling.* The computer programs MOLEDT and DISCOVER (Biosym Technologies Inc., San Diego) were used in modeling the flavin binding site. All calculations were performed on a Silicon Graphics IRIS 4D workstation.

## Results

*Spin System Assignments.* Multinuclear amino acid spin systems were assigned in concerted fashion (Oh et al., 1989; Stockman et al., 1989) by exploiting $^{13}C$- and $^{15}N$-enriched flavodoxin samples. Examples of first-order aliphatic amino acid assignments were shown previously (Stockman et al., 1989). Examples of first-order aromatic amino acid assignments are provided as supplementary material.

*Sequential Assignment of β-Sheet and Flavin Binding Site Residues.* First-order assignments were aligned sequentially by conventional techniques (Billeter et al., 1982; Wüthrich, 1986; Wüthrich et al., 1982). Sequential assignment of the five strands of the β-sheet core are shown in Figure 2. The various strands comprise the following residues (numbering corresponds to that of *A. nidulans*): $\beta_1$, residues 4–7; $\beta_2$, residues 33–36; $\beta_3$, residues 49–56; $\beta_4$, residues 81–89; $\beta_5$, residues 115–117 and 140–144. Resonances assigned to these residues exhibited NMR properties characteristic of β-sheet residues (Wüthrich, 1986): large $^3J_{N\alpha}$, as shown by the intense cross peaks in the fingerprint region of the DQF-COSY spectrum (Figure 3); weak COSY-type correlation peaks (boxed cross peaks in Figure 2) in the NOESY spectrum; intense $^1H^{\alpha}_{(i)}$–$^1H^{N}_{(i+1)}$ correlation peaks in the NOESY spectrum. Sequential connectivities for dipeptides K81–L82 and L33–H34 were not observed in spectra collected in $^1H_2O$ because the $^1H^{\alpha}$ peaks of K81 and L33 are located too close

Table I: Comparison of $^{13}C$ Chemical Shifts of FMN in Oxidized *Anabaena* 7120 Favodoxin with Those of Model Compounds[a]

| atom | *Anabaena* 7120[b] | flavin FMN[c] | TARF[c] |
|---|---|---|---|
| 2 | 158.6 | 159.8 | 155.2 |
| 4 | 161.6 | 163.7 | 159.8 |
| 4a | 135.3 | 136.2 | 135.6 |
| 5a | 135.7 | 136.4 | 134.6 |
| 6 | 129.8 | 131.8 | 132.8 |
| 7 | 141.9 | 140.4 | 136.6 |
| 7a | 20.3 | 19.9 | 19.4 |
| 8 | 152.8 | 151.7 | 147.5 |
| 8a | 23.0 | 22.2 | 21.4 |
| 9 | 117.8 | 118.3 | 115.5 |
| 9a | 130.8 | 133.5 | 131.2 |
| 10a | 152.2 | 152.1 | 149.1 |

[a] $^{13}C$ chemical shifts are relative to TMS. [b] Present study. [c] From Vervoort et al. (1986).

Table II: Selected Coupling Constants in Bound Oxidized Flavin Mononucleotide

| atoms coupled | coupling constant (Hz ± 0.5 Hz) | atoms coupled | coupling constant (Hz ± 0.5 Hz) |
|---|---|---|---|
| $^1J[^{13}C^{4}-^{13}C^{4a}]$ | 74.9 | $^1J[^{15}N^{3}-^{1}H^{3}]$ | 89.9 |
| $^1J[^{13}C^{4a}-^{13}C^{10a}]$ | 56.9 | $^3J[^{13}C^{7a}-^{1}H^{6}]$ | 5.0 |
| $^1J[^{13}C^{7}-^{13}C^{7a}]$ | 44.4 | | |
| $^1J[^{13}C^{8}-^{13}C^{8a}]$ | 41.6 | | |

to the water resonance. The sequential connectivities were observed, however, in $^2H_2O$ solution.

Sequential assignments to the residues that form the consensus binding site of the isoalloxazine ring of the cofactor (residues 92–99 and 56–59) are shown in Figure 4B. Sequential connectivities are shown beginning from the $^1H^{\alpha}$ of T56 and extending through I59 and beginning from the $^1H^{\alpha}$ of I92 and extending through Q99. Because the $^1H^{\alpha}$ signal of N58 is under the presaturated water resonance, the assignment to I59 was made on the basis of an NOE observed between $^1H^N$ of N58 and $^1H^N$ of I59. Similarly, since $^1H^{\alpha}$ of D96 also resonates near water, the D96–N97 sequential assignment stemmed from the observation of an NOE between the backbone amide protons of these two residues. Since the signals assigned to the backbone amide protons of I92, Y94, and F98 were observed in a DQF-COSY spectrum collected in $^2H_2O$ (Figure 3), these amide hydrogens exchange slowly with solvent. A summary of $^1H$ and $^{13}C$ chemical shifts for the resonances assigned here is given in supplementary Table I.

Numerous NOE connectivities between the $\beta$-strands allowed the relative orientation of each strand to be determined. As shown in Figure 5, the strands are arranged in a parallel sense. The qualitative results are consistent with the arrangement of $\beta$-sheet residues, flavin binding site residues, and the flavin cofactor observed in *A. nidulans* flavodoxin (Smith et al., 1983) as shown in Figure 6. The $\beta$-sheet forms a framework for the flavin binding site.

*Assignment of Flavin Mononucleotide $^{13}C$ and $^1H$ Resonances.* Complete assignments of flavin $^{13}C$ chemical shifts were obtained from the $^{13}C\{^{13}C\}$DQC spectrum and one-dimensional $^{13}C$ spectrum of [26% U-$^{13}C$]flavodoxin (Stockman et al., 1988b). All three carbon spin systems of the cofactor were assigned (xylene ring, $^{13}C^{4}-^{13}C^{4a}-^{13}C^{10a}$, and ribityl group). One-bond $^{13}C-^{13}C$ coupling constant information was extracted from well-resolved regions in this spectrum. As expected, the isolated $^{13}C^2$ carbonyl carbon of FMN showed no correlations in the double quantum spectrum but was identified readily in the one-dimensional spectrum. Flavin $^{13}C$ chemical shifts and selected $^{13}C-^{13}C$ coupling constants are summarized in Tables I and II, respectively. $^{13}C$ assignments were extended to the resonances of attached aromatic and aliphatic protons. Assignment of the flavin proton signals was a prerequisite to NOESY experiments that utilized FMN as a binding-site probe (see below).

Table III: Observed Protein–Flavin Mononucleotide NOEs

| flavin proton(s) | protein proton(s) | flavin proton(s) | protein proton(s) |
|---|---|---|---|
| 3 | T56 $\beta$, $\gamma$ | 7a | W57 $\epsilon_3$, $\zeta_3$ |
| | G60 N | 8a | W57 $\zeta_3$, $\eta_2$ |
| | Y94 $\alpha$, $\beta_1$, $\beta_2$ | 2′ | G89 $\alpha$ |
| | N97 N, $\alpha$, $\beta_1$, $\beta_2$ | 3′ | G89 $\alpha$ |
| | F98 $\alpha$ | 4′ | P55 $\alpha$ |
| | Q99 N | | W57 $\zeta_2$ |
| 6 | W57 $\epsilon_3$, $\zeta_3$ | 5′ | W57 $\zeta_2$ |
| | N58 N | | |
| | I59 N | | |

Table IV: Observed FMN–FMN NOEs

| FMN proton(s) | FMN proton(s) |
|---|---|
| 6 | 7a |
| 9 | 8a |
| 1′ | 9 |
| 2′ | 1′, 1″, 9′ |
| 3′ | 1′, 1″ |

*Identification of Resonances from Amino Acids in the Flavin Binding Site.* NOEs from the resolved flavin $N^3$ proton at 10.54 ppm (Stockman et al., 1988a) provided a wealth of information regarding residues in the vicinity of this edge of the isoalloxazine ring. Figure 4A shows several assigned NOEs from the $N^3$ proton to residues in the 56–59 and 92–99 segments. These indicate short distances (<5 Å) to the $N^3$ proton. Unfortunately, $^1H^{N3}$ was the only flavin proton resolved in 1D spectra.

To overcome the resolution problem, $^1H\{^{13}C\}$SBC-NOE spectra were recorded. The addition of the $^{13}C$ chemical shift dispersion greatly improved spectral resolution and permitted simplified and more confident data analysis. Figure 7 shows the region of the $^1H\{^{13}C\}$SBC-NOE spectrum that contains NOE signals arising from the ribityl side chain protons. The numbers 2′, 3′, 4′, and 5′ identify the ribityl one-bond $^1H-^{13}C$ correlations. NOEs that arise from a given ribityl proton lie along a horizontal line from the direct peak. Both intraflavin and flavin–protein NOEs were observed. A spin system classified as a glycine, but unassigned sequentially, was assigned to G89 on the basis of its NOEs to ribityl protons 2′ and 3′ (Figure 7). G89 is the glycine nearest to the ribityl 2′ and 3′ protons in the crystal structure of *A. nidulans* (Smith et al., 1983). Figure 8 shows a region of the $^1H\{^{13}C\}$SBC-NOE spectrum that contains NOEs between ring protons of W57 and the two methyl groups of the isoalloxazine ring. Assignments are indicated at the positions of the one-bond $^1H-^{13}C$ peaks. Figure 8A contains NOEs from the methyl groups to the W57 protons; Figure 8B contains NOEs from the W57 protons to the flavin methyl groups. A total of 25 protein–FMN NOEs (Table III) and 8 intra-FMN NOEs (Table IV) have been identified.

*Determination of $^3J(C^{7a}H^{6})$ in Bound FMN.* Heteronuclear three-bond coupling constants can be correlated with molecular conformation. Recently, Montelione et al. (1989) presented a simple procedure for the accurate measurement of heteronuclear coupling constants in $^1H\{^1H\}$ spectra of $^{13}C$- or $^{15}N$-enriched proteins. The technique relies on the observation of a correlation (scalar or dipolar) between two protons that are each scalar coupled to the same heteronucleus. In our case, [26% U-$^{13}C$ FMN]flavodoxin was used as the sample, and

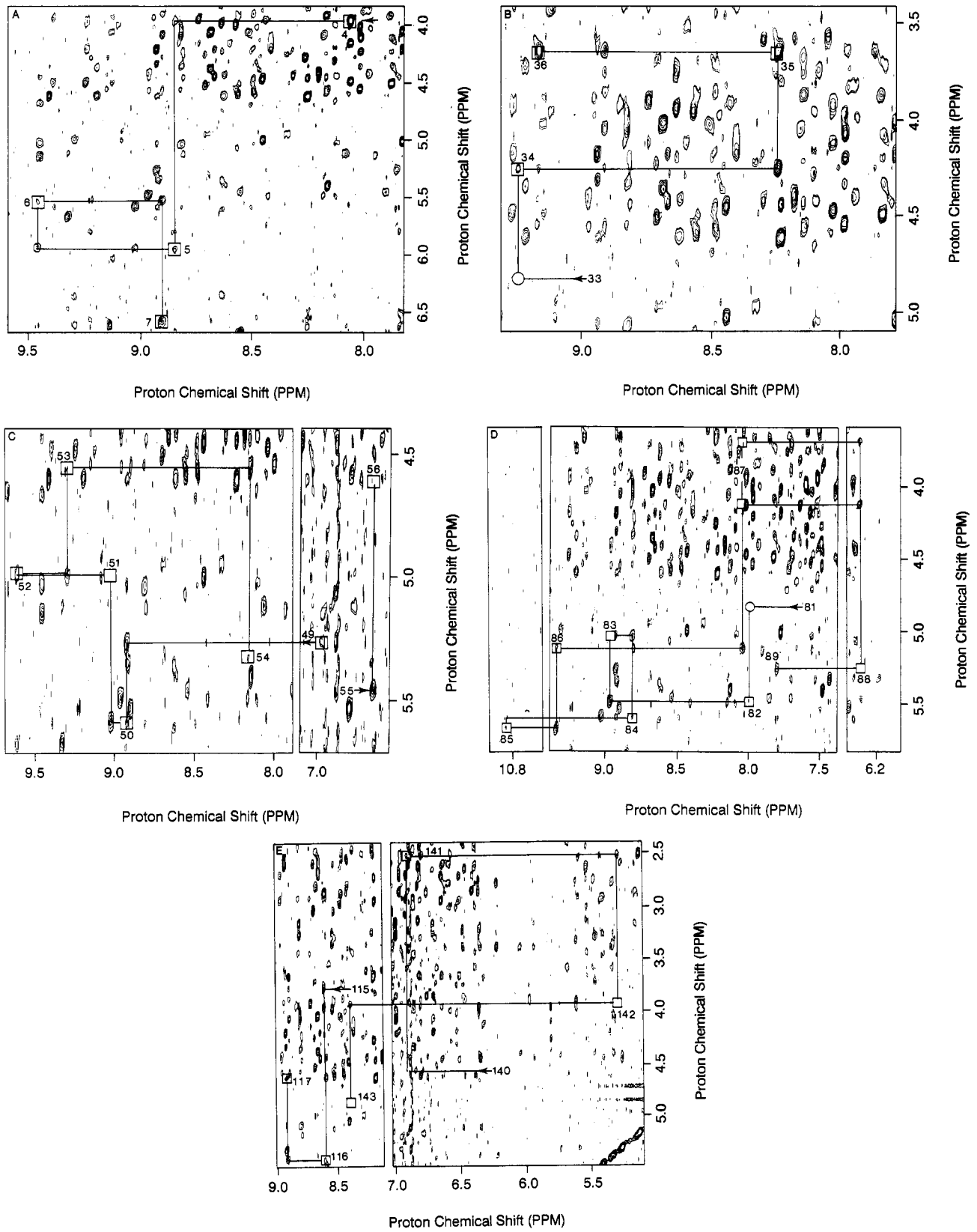


FIGURE 2: Portions of the NOESY spectrum of oxidized flavodoxin at 600 MHz showing sequential assignments for each of the five strands in the parallel $\beta$-sheet: (A) $\beta_1$, residues 4–7; (B) $\beta_2$, residues 33–36; (C) $\beta_3$, residues 49–56; (D) $\beta_4$, residues 81–89; (E) $\beta_5$, residues 115–117 and 140–144. The convention of Wagner et al. (1986) is used in which boxes indicate COSY-type cross peaks. The sample was 8 mM flavodoxin in 90% $^1H_2O$/10% $^2H_2O$. The sweep width was 8928 Hz; the 90° pulse width was 7.2 $\mu$s. The mixing time was 250 ms. Presaturation was used during the 1.8-s relaxation delay to eliminate the water resonance. A total of 448 blocks were collected; each was the average of 48 free induction decays (4096 data points each).

$^{13}C$-editing was exploited so that the NOESY spectrum contained peaks only from NOE interactions originating from the FMN group. This removed resonance overlaps from protein–protein NOEs. Figure 9 shows NOEs from the flavin 7a (2.83 ppm) and 8a (2.77 ppm) methyl protons to the W57 $\zeta_3$ proton (7.09 ppm) and from the flavin 7a methyl protons to the flavin 6 proton (7.55 ppm). No $^{13}C$ decoupling was used in either dimension. The large splitting in the vertical di-

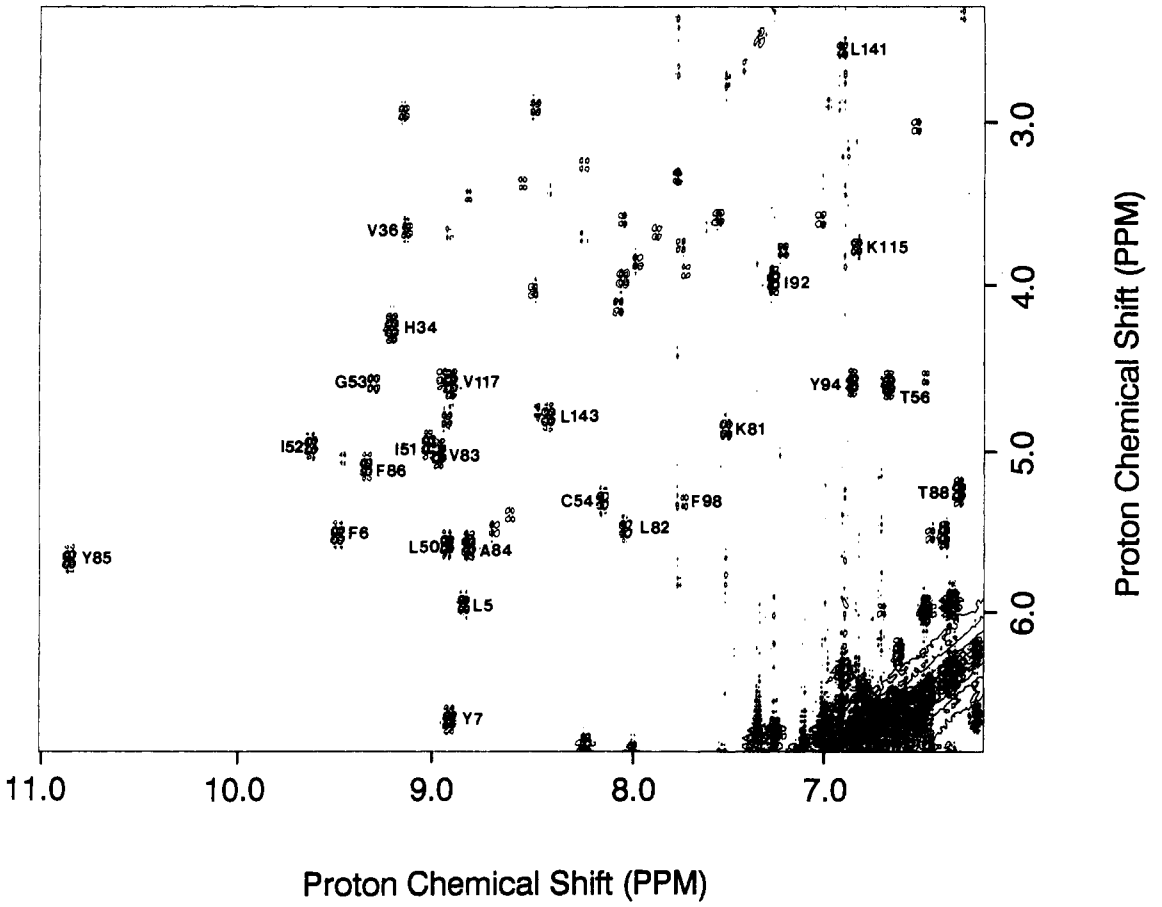


FIGURE 3: Region of the 600-MHz DQF-COSY spectrum of oxidized flavodoxin in $^2H_2O$. Only those amide groups that undergo slow hydrogen exchange give rise to cross peaks under these conditions. Resonances assigned to residues involved in the $\beta$-sheet structure or the flavin binding site are indicated. The sample was 8 mM flavodoxin in 100% $^2H_2O$. The sweep width was 8928 Hz, the 90° pulse width was 7.1 $\mu$s, and the relaxation delay was 2 s. A total of 512 blocks were collected; each was the average of 64 free induction decays (2048 data points each).

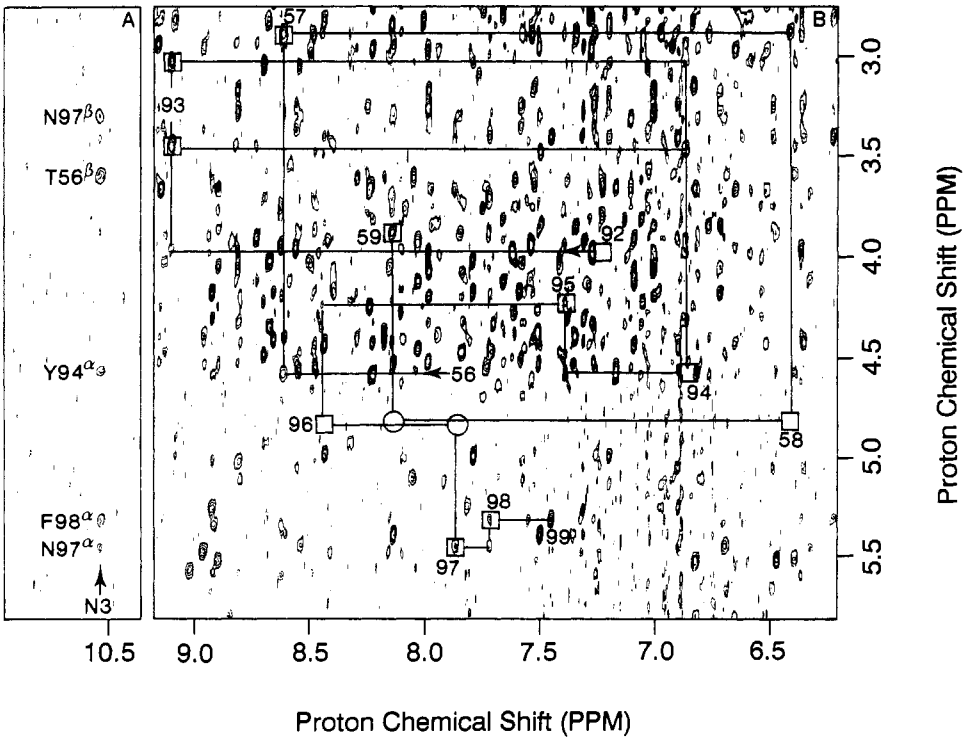


FIGURE 4: Portion of the NOESY spectrum of oxidized flavodoxin at 600 MHz. (A) Assignment of NOEs observed involving the $N^3$ proton of the isoalloxazine ring. (B) Sequential assignment of residues 56–59 and 92–99. Sample conditions and figure annotations were as described in the legend to Figure 2.

mension results from single-bond proton–carbon coupling ($^1J_{CH}$). The weaker splitting in the horizontal dimension arises from multiple-bond proton–carbon coupling. By measuring the horizontal separation between the two NOE peaks assigned

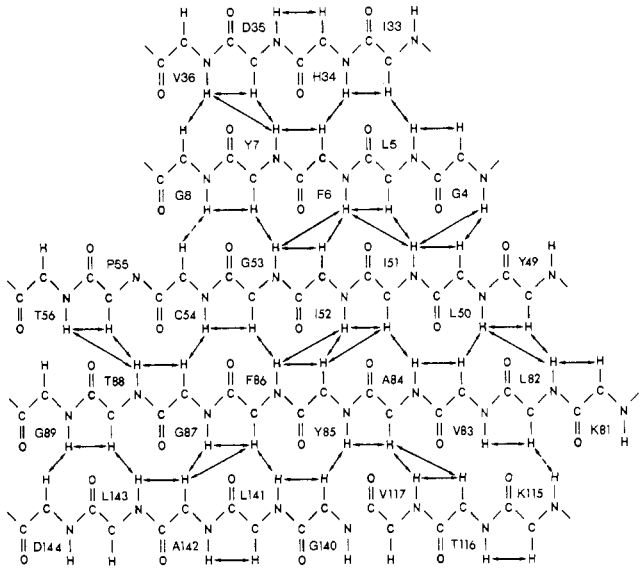


FIGURE 5: Summary of observed sequential and interstrand NOEs used to define the orientation of the parallel $\beta$-sheet structure. Dashed lines indicate possible NOE connectivities that are obscured by overlapping cross peaks.

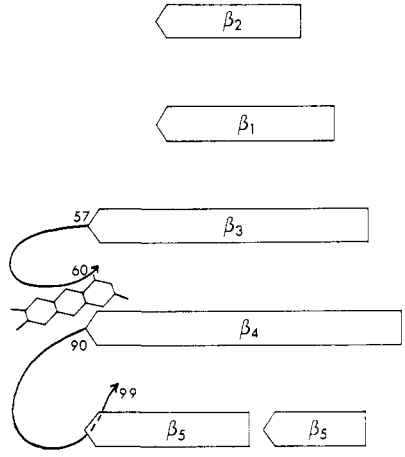


FIGURE 6: Schematic diagram illustrating how the $\beta$-sheet structure forms a framework about which the flavin binding site is arranged.

to the interaction between the flavin 7a methyl and the $^1H^6$, one obtains the three-bond heteronuclear coupling constant (5.0 Hz) between $^{13}C^{7a}$ and $^1H^6$. The NOE peaks assigned to interactions between W57 protons and flavin methyl protons do not show a horizontal separation because they are not coupled to a common heteronucleus. Unfortunately, the NOE between $^1H^{8a}$ and $^1H^9$ was not strong enough to permit determination of the three-bond coupling between $^{13}C^{8a}$ and $^1H^9$. In addition, a $^{13}C^{8a}$–$^1H^9$ correlation was not observed in the $^1H\{^{13}C\}$MBC spectrum shown in Figure 10. By contrast, a strong $^{13}C^{7a}$–$^1H^6$ correlation was seen.

*Observation of Tyrosine 94 Exchange Peaks.* Figure 11 shows the aromatic region of a mixed NOESY–ROESY ("pure-exchange") spectrum acquired with the pulse sequence of Fejzo et al. (1990). This experiment provides cross peaks only from groups that undergo exchange on a time scale faster than $^1H$ relaxation but slower than the inverse of the chemical shift difference in hertz. The resonances seen in Figure 11 correspond to the $\delta$- and $\epsilon$-protons of Y94. As a result of the slow ring flip, distinct $^1H$ and $^{13}C$ chemical shifts are observed for $\delta_1$ and $\delta_2$ and $\epsilon_1$ and $\epsilon_2$.

*Molecular Modeling.* Distance constraints derived from NOE data were used to determine the local solution structure of the FMN binding site. Cross-peak intensities from NOESY

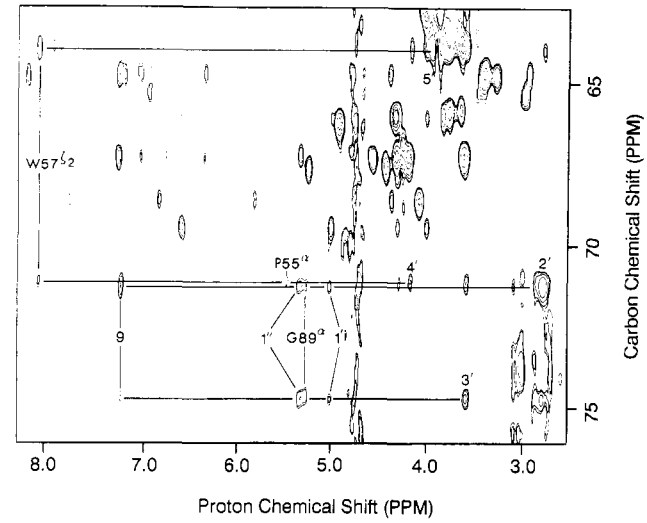


FIGURE 7: Region of the 600-MHz $^1H\{^{13}C\}$SBC-NOE spectrum of oxidized flavodoxin. NOEs arising from the ribityl protons (2′, 3′, 4′, and 5′) are identified. The sample was 7 mM [26% U-$^{13}C$]flavodoxin in 100% $^2H_2O$. A total of 256 blocks were collected; each was the average of 128 free induction decays (2048 data points each). The 90° proton pulse was 8.6 $\mu$s; the 90° carbon pulse was 44 $\mu$s. The proton sweep width was 8 928 Hz, and the carbon sweep width was 10 638 Hz. The carbon sweep width covered only the aliphatic region of the spectrum. The aromatic region was recorded separately. The NOE mixing time was 200 ms.

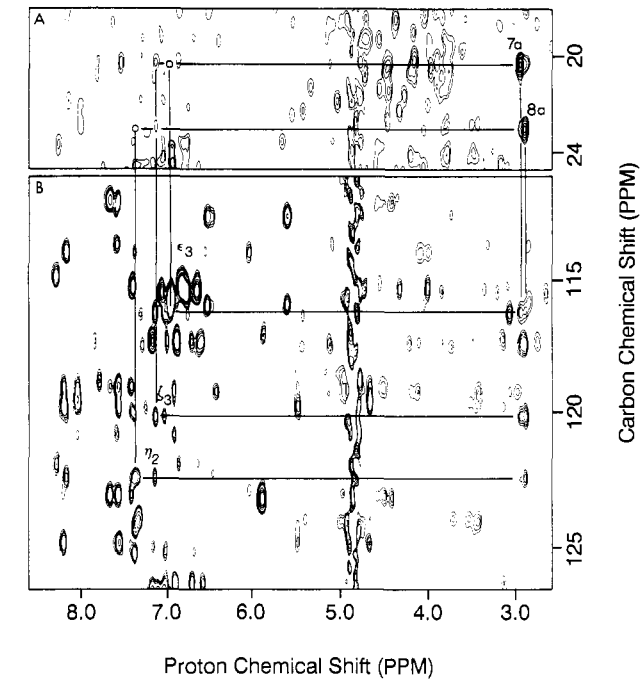


FIGURE 8: Aliphatic (A) and aromatic (B) regions of $^1H\{^{13}C\}$SBC-NOE spectra of oxidized flavodoxin. NOEs from the two flavin methyl groups to tryptophan 57 ring protons are shown in (A). Circles indicate the positions of NOE peaks that are too weak to be seen at the level plotted. Confirmatory NOEs from tryptophan 57 ring protons to the flavin methyl groups are shown in (B). Sample conditions and acquisition parameters were as described in the legend to Figure 7, except that the NOE mixing time in (B) was 250 ms.

spectra recorded with mixing times between 50 and 250 ms were classified into six categories to give upper distance limits: strong, 2.2 Å; medium-strong, 2.6 Å; medium, 3.0 Å; medium-weak, 3.5 Å; weak, 4.0 Å; very weak, 5.0 Å. Refined X-ray crystallography coordinates of the 70% homologous flavodoxin from *A. nidulans* (Dr. M. L. Ludwig, personal communication) were used as the starting point. The molecular editing program MOLEDT was used to replace non-

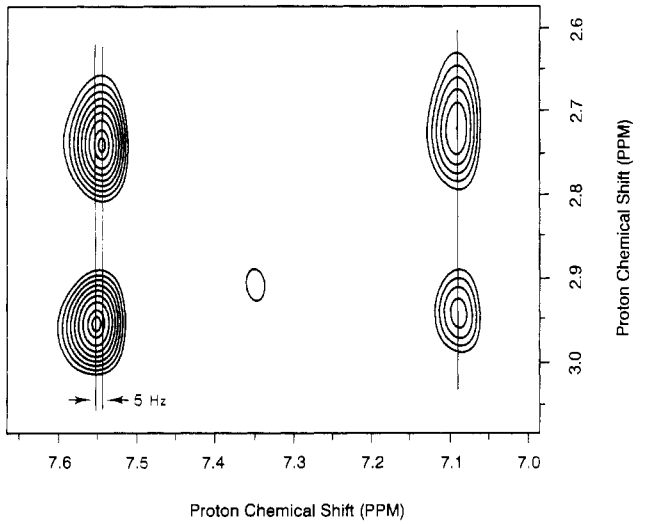


FIGURE 9: $^{13}C$-Edited $^1H\{^1H\}$NOESY spectrum at 600 MHz oxidized flavodoxin. The sample was 4 mM [26% U-$^{13}$CFMN]flavodoxin in 100% $^2H_2O$. The 90° proton pulse was 9.5 μs, and the 90° carbon pulse was 19 μs. The sweep width was 8928 Hz. Presaturation during the 2-s relaxation delay was used to remove the residual $^1H^2HO$ resonance. A total of 256 blocks were collected; each was the average of 256 free induction decays (2048 data points each). The NOE mixing time was 250 ms. After Fourier transformation, the program ZOOM (Z. Zolnai, S. Macura, and J. L. Markley, unpublished results) was used to cut out the region of interest, back Fourier transform it, zero fill it, and Fourier transform it again. This gave a final resolution of 0.517 Hz/point in $\omega_2$.

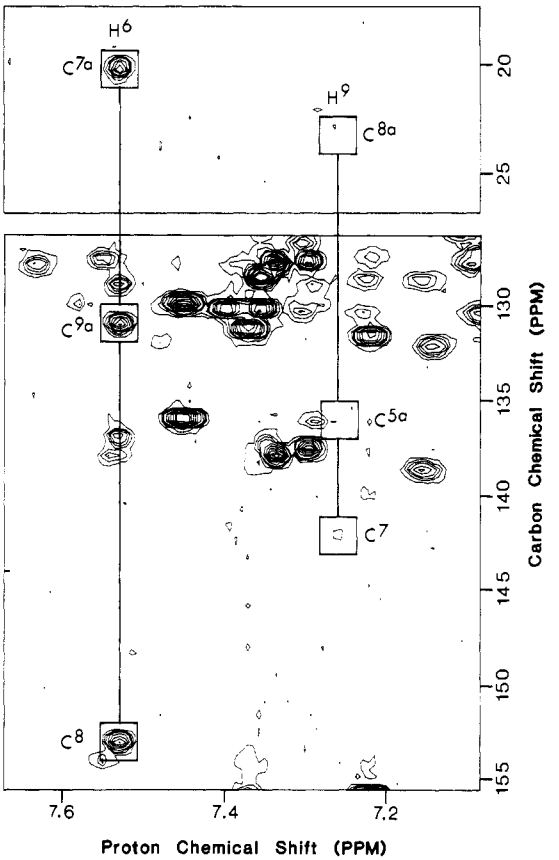


FIGURE 10: Region of the $^1H\{^{13}C\}$MBC spectrum (14.2 T) of flavodoxin. Sample conditions were as described in the legend to Figure 7. A total of 512 blocks were collected; each contained the average of 64 free induction decays (4096 data points each). The 90° proton pulse was 8.4 μs; the 90° carbon pulse was 12.4 μs. The proton sweep width was 8928 Hz, and the carbon sweep width was 27 778 Hz. The delay time used to suppress one-bond couplings was 3.57 ms. The delay time used to optimize for 7-Hz carbon–proton couplings was 70 ms. The acquisition time was 0.299 s, and the relaxation delay was 2 s.

conserved residues. Maximum primary sequence alignment was maintained by inserting a glycine at position 29 in the sequence of *Anabaena* 7120 flavodoxin (Figure 1). MOLEDT also was used to build an FMN molecule that contained partial atomic charges as defined by Vinayaka and Rao (1984). The program DISCOVER was used to minimize the energy of this structure. Energy minimization consisted of 500 steepest descent iterations followed by 5000 conjugate gradient iterations. The resulting structure was then subjected to restrained energy minimization calculations. Five intra-FMN, 22 FMN–protein, and 29 intraprotein NOE-derived distance constraints were incorporated into the calculations. A square-well harmonic function (Clore et al., 1986) was used to restrain the NMR-derived distances. The left and right force constants were set to 25.15 kcal/(mol·Å). Energy penalties were applied for distances shorter than the van der Waals contact radii or longer than the NOE-derived distance. Average proton positions for methylene and methyl groups were used. Calculations were limited to residues within 12 Å of $C^{2'}$ of FMN (Vinayaka & Rao, 1984). This included residues 8–17, 53–63, 86–102, and 142–147. All other residues remained fixed during the restrained energy minimization calculations. Only three of the NMR-constrained distances had violations greater than 0.1 Å. None of these three was larger than 0.3 Å. The final structure is shown in Figure 12, which displays only the flavin group and nonfixed amino acid residues considered in the restrained energy minimization calculations. Restrained molecular dynamics calculations in combination with restrained energy minimization calculations yielded structures very similar to those obtained by using only restrained energy minimization.

## DISCUSSION

*β-Sheet and Flavin Binding Site Structure.* The NMR data for *Anabaena* 7120 flavodoxin show that the β-sheet is composed of five parallels strands. Their arrangement is very similar to that observed in the crystal structure of the 70% homologous long-chain flavodoxin from *A. nidulans* (Smith et al., 1983; Laudenbach et al., 1987). The present assignments include all β-sheet residues expected on the basis of the crystal structure of *A. nidulans* flavodoxin except resonances from residues 30–32, 2–3, and 48, which remain unassigned. These residues are located adjacent to each other in one corner of the β-sheet.

Two loops of the protein form the flavin ring binding site. The β-sheet structure serves as a framework for these binding site residues, as shown in Figure 6. Interactions between the cofactor and flavin binding site residues are shown in Figure 12. The flavin ring is bracketed by the ring systems of W57 and Y94. The relative orientation of the flavin, tryptophan, and tyrosine rings observed in *Anabaena* 7120 flavodoxin is similar to that observed in *A. nidulans* (Laudenbach et al., 1987). The indole ring of W57 is more coplanar with the flavin ring in *A. nidulans* flavodoxin than in *Anabaena* 7120 flavodoxin; in the latter, the outer edge of the benzene ring is pointed toward the flavin methyl groups. The tyrosine ring overlaps the flavin ring slightly less in *Anabaena* 7120 than in *A. nidulans* flavodoxin, but is still positioned to form good ring stacking interactions. The reduced ring flip rate observed for Y94 can be explained by hydrophobic interactions with the flavin ring system and with the side chain of I59.

Numerous hydrogen bonds between the protein and the flavin cofactor have been identified. Hydrogen bonds exist between the ribityl phosphate oxygens and the backbone amide

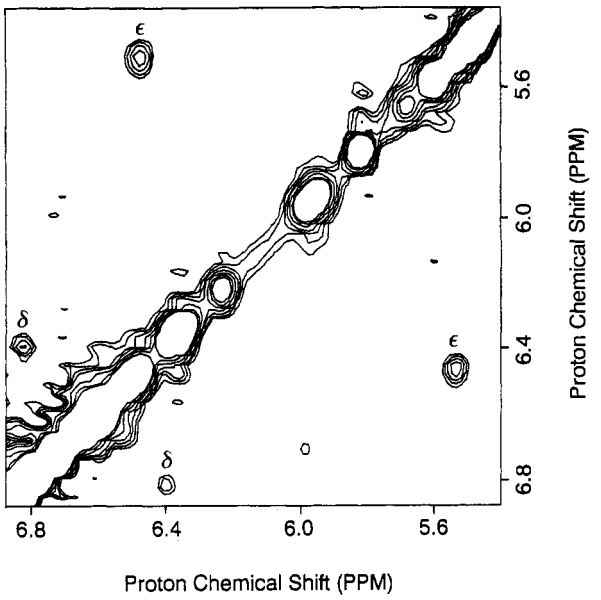


FIGURE 11: Region of the mixed NOESY–ROESY spectrum at 500 MHz of oxidized flavodoxin. Exchange peaks are shown for the $^1H^{\delta}$ and $^1H^{\epsilon}$ of tyrosine 94. Sample conditions were as described in the legend to Figure 2. A total of 512 blocks, each containing the average of 64 free induction decays (4096 data points each), were collected. The sweep width was 15 151 Hz, and the 90° pulse width was 21 μs. The data were collected by using pulse sequence C from Fejzo et al. (1990). The 50-ms mixing time consisted of 2 parts NOE and 1 part ROE.

protons of Q10, T11, G12, K13, T14; the side-chain hydroxyl protons of T9, T11, and T14; and the $\epsilon_1$-proton of W57. The ribityl 2′-hydroxyl group is positioned to form hydrogen bonds with the main-chain carbonyl oxygens of T56 and T88 and the backbone amide proton of T56. A hydrogen bond was also identified between the ribityl 4′-hydroxyl group and the side-chain hydroxyl group of T88. These interactions, which are very similar to those observed in *A. nidulans* flavodoxin (Smith et al., 1983; Laudenbach et al., 1987), are consistent with the hypothesis that the ribityl side chain functional groups help anchor the cofactor into the protein. Both carbonyl oxygens of the flavin ring appear to hydrogen bond to binding-site residues: $O^{C2}$ to the backbone amide protons of D90 and Q99; $O^{C4}$ to the backbone amide proton of G60. In addition, $H^{N3}$ forms a strong hydrogen bond to the main-chain carbonyl oxygen of N97. $N^5$ may be weakly hydrogen bonded to the backbone amide proton of I59, but this interaction probably does not account for the unusual chemical shift observed for this nitrogen (see below). No hydrogen bonds were observed to $N^1$.

*Electronic Environment of Bound FMN.* Insights into the electronic environment and conformation of the bound cofactor can be obtained from spectral properties of the isoalloxazine ring system. These include $^{13}C$ and $^{15}N$ chemical shifts (Moonen et al., 1984a; Vervoort et al., 1986), $^{13}C$–$^{13}C$ coupling constants (Vervoort et al., 1986), and $^{13}C$–$^1H$ coupling constants.

Table I compares $^{13}C$ chemical shifts determined for protein-bound FMN with those determined for FMN in polar and for TARF in apolar environments. The $^{13}C^2$ and $^{13}C^4$ chemical shifts of flavodoxin fall between those observed in model compounds in polar and apolar environments. This suggests that the carbonyl oxygens of these two carbons may participate in hydrogen bonds. This hypothesis is supported by the experimental one-bond $^{13}C^4$–$^{13}C^{4a}$ and $^{13}C^{4a}$–$^{13}C^{10a}$ coupling constants (Table II), which resemble more closely those of FMN in a polar solvent than TARF in an apolar solvent. The $^{15}N$ chemical shifts reported earlier (Stockman et al., 1988a) also suggested that this edge of the flavin ring is polarized by interactions with residues in the flavin binding site. In addition, the one-bond $^{15}N^3$–$^1H^3$ coupling constant (Table II), measured from the splitting of $^1H^{N3}$ in the one-dimensional $^1H$ NMR spectrum of [95% U–$^{15}N$]flavodoxin, along with the slow exchange of $^1H^{N3}$ with solvent (Stockman et al., 1988a) indicates that this position is hydrogen bonded to the protein. The local structure of the FMN binding site (Figure 12) indicates that the backbone amide protons of G60 (to $O^{C4}$) and D90 and Q99 (to $O^{C2}$) and the main-chain carbonyl oxygen of N97 (to $H^{N3}$) are responsible for these hydrogen bonds.

Hydrogen bonding to the FMN carbonyl groups has been shown to result in upfield shifts in the resonances of $C^8$, $C^6$, $N^5$, $C^{9a}$, and $C^{10a}$. These effects can be partially offset by increased $sp^2$ hybridization of $N^{10}$, which results in downfield shifts in the resonances of $C^9$, $C^7$, $C^{7a}$, and $C^{5a}$ and an upfield shift in the resonance of $C^{4a}$ (Moonen et al., 1984; Vervoort et al., 1986). The chemical shifts of the remaining flavin ring carbon atoms (with the exception of $C^6$ discussed below) as well as that of $N^{10}$ (Stockman et al., 1988) resemble those observed in *Azotobacter vinelandii* flavodoxin (Vervoort et al.,

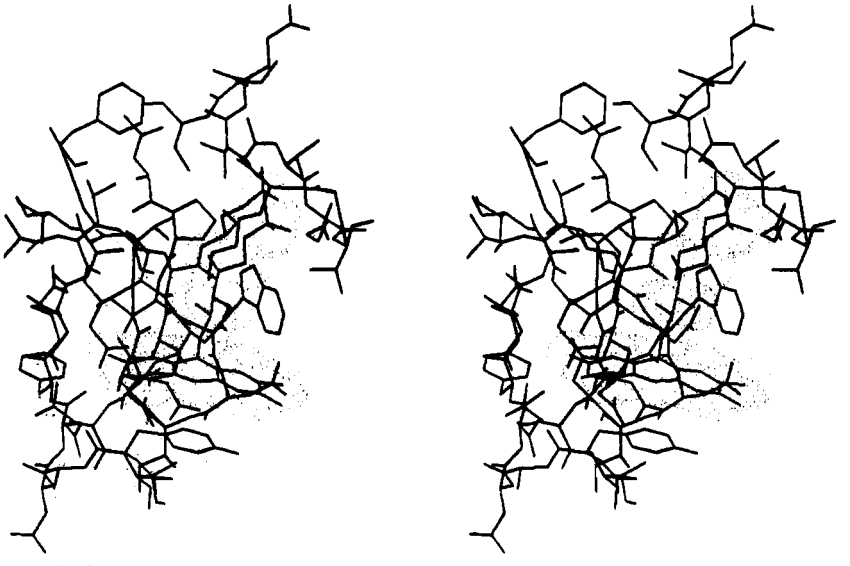

FIGURE 12: Stereoview of the NOESY distance-constrained energy-minimized structure of the flavin mononucleotide bonding site in oxidized *Anabaena* 7120 flavodoxin. Van der Waals radii are shown for the FMN group.

1986) more closely than they do those of other flavodoxins studied. When ring-current effects from the adjacent tryptophan 57 in *Anabaena* 7120 are taken into account (there is no aromatic residue at this position in *A. vinelandii* flavodoxin), the correspondence of carbon chemical shifts is even greater. In this regard, it is interesting to note that the oxidized-semiquinone redox potentials for these two flavodoxins differ by only 30 mV and that they are both more negative by at least 80 mV than those of the three other flavodoxins for which NMR chemical shifts have been reported (*Desulfovibrio vulgaris*, *Megasphaera elsdenii*, and *Clostridium MP*) (Vervoort et al., 1986).

Earlier we reported that the chemical shift of $^{15}N^5$ of *Anabaena* 7120 flavodoxin closely resembles that of free FMN in solution and suggested that $^{15}N^5$ may be hydrogen bonded to water (Stockman et al., 1988a). A similar FMN-like chemical shift was observed for $^{15}N^5$ in the bound FAD of 6-hydroxy-L-nicotine oxidase from *Arthrobacter oxidans* and was attributed to hydrogen bonding of this nitrogen to a water molecule (Pust et al., 1989). By contrast, the $^{15}N^5$ chemical shift of most other flavodoxins studied differs from that of FMN by about 6 ppm. This suggests that $N^5$ of the other flavodoxins is much more weakly hydrogen bonded (Vervoort et al., 1986) than that of *Anabaena* 7120 flavodoxin. Similarly, the chemical shift of $^{13}C^6$ of *Anabaena* 7120 flavodoxin resonates 3 ppm farther upfield from those of other flavodoxins; it more closely resembles the chemical shift of free FMN in solution than do those of other flavodoxins. Taken together, the observed chemical shifts of $^{15}N^5$ and $^{13}C^6$ suggest that this edge of the flavin ring is solvent accessible in *Anabaena* 7120 flavodoxin. The solvent-accessible surface area calculated for the structure shown in Figure 12 indicates that $C^6$ is solvent accessible but that $N^5$ is not. Since the model was constructed without consideration of water molecules, a small structural change to accommodate a water molecule cannot be ruled out. A bound water molecule could be stabilized by hydrogen bonds to $N^5$ and to the backbone amide protons of N58 and I59.

*Distortion of the Flavin Xylene Ring.* The oxidized flavin isoalloxazine ring system contains 16 $\pi$-electrons and thus is not formally aromatic. This presents the possibility that portions of the three-ring system may not be coplanar and that protein–cofactor interactions involving one part of the isoalloxazine ring may influence the chemistry that occurs elsewhere in the ring system (Hall et al., 1987). Bending about the $N^5$–$N^{10}$ bond has been shown to occur (Moonen et al., 1984a; Hall et al., 1987) and may account partially for modulation of the FMN redox potential by the protein.

Distortions also may occur in the xylene ring moiety. $^1H$ NMR data for a series of isoalloxazine ring systems indicate that methyl substitutions may distort the benzene-like ring (Grande et al., 1977a,b). The distortions may result in the xylene ring becoming less aromatic and may contribute to modulation of the redox potentials (Hall et al., 1987). In addition, computed changes in the partial atomic charges between the reduced and oxidized states of lumiflavin indicated that the xylene ring acts as a polarizability source for changes occurring in the redox-active diazadiene region (Hall et al., 1987). The xylene ring also has been proposed to be involved in redox potential manipulation in flavoproteins that contain covalently bound FMN or FAD (Williamson & Edmondson, 1985). In these proteins, the amino acid side-chain substituent forming the covalent bond to the $C^{8a}$ methyl group may influence the redox potentials.

The observed one-bond ($^{13}C$–$^{13}C$) and three-bond ($^{13}C$–$^1H$) coupling constants (Table II) suggest that the flavin xylene ring in *Anabaena* 7120 flavodoxin is distorted from planarity. Angle-dependent (Karplus & Karplus, 1972) three-bond correlations in the $^1H\{^{13}C\}$MBC spectrum (Figure 10) indicate that the distortion is localized to the $C^8$–$C^9$–$C^{9a}$ region of the ring. Strong correlations are observed between $^1H^6$ and $^{13}C^8$, $^{13}C^{9a}$, and $^{13}C^{7a}$. These observations, as well as the 5-Hz coupling measured between $^1H^6$ and $^{13}C^{7a}$ (Table II), are expected for a planar geometry. By contrast, the only multiple-bond correlation seen from $^1H^9$ to xylene carbon atoms was the very weak one to $^{13}C^7$. Three-bond $^1H^9$–$^{13}C^{5a}$ and $^1H^9$–$^{13}C^{8a}$ correlations were not observed. Lack of three-bond correlations is expected if the geometry is distorted from planarity. Distortion of the $C^8$–$C^9$–$C^{9a}$ region would result in a larger distance between $^1H^{8a}$ and $^1H^9$. This is supported by NOE data: a very weak NOE was seen between $^1H^{8a}$ and $^1H^9$, while a strong NOE was seen between $^1H^{7a}$ and $^1H^6$ (Figure 9). Finally, the $^{13}C^7$–$^{13}C^{7a}$ coupling (44.4 Hz) is that expected for a methyl group on an aromatic ring. The smaller $^{13}C^8$–$^{13}C^{8a}$ coupling (41.6 Hz) suggests that $C^8$ is less aromatic than $C^7$.

## Conclusion

The local structure of the flavin binding site in *Anabaena* 7120 flavodoxin is very similar to that observed in *A. nidulans* flavodoxin. It is not surprising, then, that the redox potentials for these two proteins are very similar (Paulsen et al., 1990). $E_1$ and $E_2$ for the two flavodoxins differ by only 25 mV, with both values less negative for *Anabaena* 7120 flavodoxin than for *A. nidulans* flavodoxin. Structure–function relationships responsible for modulation of the FMN redox potentials in flavoproteins are still poorly understood. Contributions from charge–charge interactions, changes in hydrogen bonding, and flavin ring distortion are thought to be involved, but their correlation with redox potentials is hampered by the limited number of structures available. The results presented here lay the groundwork for site-directed-mutagenesis studies (in progress) aimed at assessing the changes in redox potential that occur with changes in the structure of the FMN binding site. In addition, the X-ray structure of *Anabaena* 7120 flavodoxin soon will be available for comparison (M. Sundaralingam, personal communication).

## Acknowledgments

We thank Dr. David W. Krogmann (Purdue University) for advice on isolating the flavodoxin and Dr. Martha Ludwig (University of Michigan) for graciously supplying refined coordinates of the crystal structure of *A. nidulans* prior to publication and for stimulating discussions. We also thank Dr. Ed S. Mooberry for optimizing NMR instrumentation and Drs. W. Milo Westler and Prashanth Darba for helpful discussions.

## Supplementary Material Available

Figures (five) showing examples of proton and carbon resonance assignments to aromatic amino acids and flavin mononucleotide and tables (two) of assigned proton, carbon, and nitrogen chemical shifts of $\beta$-sheet and flavin binding site residues and summary of energy minimization output including distance constraints and residual violations (15 pages). Ordering information is given on any current masthead page.

**Registry No.** FMN, 146-17-8.

## References

Anil Kumar, Ernst, R. R., & Wüthrich, K. (1980) *Biochem. Biophys. Res. Commun. 95*, 1–6.

Bax, A., & Summers, M. F. (1986) *J. Am. Chem. Soc. 108*, 2093–2094.

Bax, A., Griffey, R. H., & Hawkins, B. L. (1983) *J. Magn. Reson. 55*, 301–315.

Billeter, M., Braun, W., & Wüthrich, K. (1982) *J. Mol. Biol. 155*, 321–346.

Bodenhausen, G., Kogler, H., & Ernst, R. R. (1984) *J. Magn. Reson. 58*, 370–388.

Clore, G. M., Brünger, A. T., Karplus, M., & Gronenborn, A. M. (1986) *J. Mol. Biol. 191*, 523–551.

Fejzo, J., Westler, W. M., Macura, S., & Markley, J. L. (1990) *J. Am. Chem. Soc. 112*, 2574–2577.

Grande, H. J., van Schagen, C. G., Jarbandhan, T., & Müller, F. (1977a) *Helv. Chem. Acta 60*, 348–368.

Grande, H. J., Gast, R., van Schagen, C. G., van Berkel, W. J. H., & Müller, F. (1977b) *Helv. Chem. Acta 60*, 367–379.

Hall, L. H., Bowers, M. L., & Durfor, C. N. (1987) *Biochemistry 26*, 7401–7409.

Harper, C. (1988) A Comparative Study of Proteins Isolated from *Microcystis aeruginosa*, M.S. Thesis, Purdue University, West Lafayette, IN.

Karplus, S., & Karplus, M. (1972) *Proc. Natl. Acad. Sci. U.S.A. 69*, 3204–3206.

Laudenbach, D. E., Straus, N. A., Pattridge, K. A., & Ludwig, M. L. (1987) in *Flavins and Flavoproteins* (Edmondson, D. E., & McCormick, D. B., Eds.) pp 249–260, Walter de Gruyter, New York.

Leonhardt, K. G., & Straus, N. A. (1989) *Nucleic Acids Res. 17*, 4384.

Levitt, M. H., & Ernst, R. R. (1983) *Mol. Phys. 50*, 1109–1124.

Mayhew, S. G. (1971) *Biochim. Biophys. Acta 235*, 289–302.

Mayhew, S. G., & Ludwig, M. L. (1975) *Enzymes (3rd Ed.) 12*, 57–118.

Montelione, G. T., Winkler, M. E., Rauenbuehler, P., & Wagner, G. (1989) *J. Magn. Reson. 82*, 198–204.

Moonen, C. T. W., Vervoort, J., & Müller, F. (1984) *Biochemistry 23*, 4859–4867.

Oh, B.-H., Westler, W. M., & Markely, J. L. (1989) *J. Am. Chem. Soc. 111*, 3083–3085.

Paulsen, K. E., Stankovich, M. T., Stockman, B. J., & Markely, J. L. (1990) *Arch. Biochem. Biophys. 280*, 68–73.

Pust, S., Vervoort, J., Decker, K., Bacher, A., & Müller, F. (1989) *Biochemistry 28*, 516–521.

Rance, M., Sørensen, O. W., Bodenhausen, G., Wagner, G., Ernst, R. R., & Wüthrich, K. (1983) *Biochem. Biophys. Res. Commun. 117*, 479–485.

Shaka, A. J., Keeler, J., Frenkiel, T., & Freeman, R. (1983) *J. Magn. Reson. 52*, 335–338.

Simondson, R. P., & Tollin, G. (1980) *Mol. Cell. Biochem. 33*, 13–24.

Smith, W. W., Pattridge, K. A., Ludwig, M. L., Petsko, G. A., Tsernoglou, D., Tanaka, M., & Yasunobu, K. T. (1983) *J. Mol. Biol. 165*, 737–755.

Stockman, B. J., & Markley, J. L. (1990) in *Advances in Biophysical Chemistry* (Bush, C. A., Ed.) (in press).

Stockman, B. J., Westler, W. M., Mooberry, E. S., & Markley, J. L. (1988a) *Biochemistry 27*, 136–142.

Stockman, B. J., Westler, W. M., Darba, P., & Markley, J. L. (1988b) *J. Am. Chem. Soc. 110*, 4095–4096.

Stockman, B. J., Reily, M. D., Westler, W. M., Ulrich, E. L., & Markley, J. L. (1989) *Biochemistry 28*, 230–236.

Sykes, G. A., & Rogers, L. J. (1984) *Biochem. J. 217*, 845–850.

Tollin, G., & Edmondson, D. E. (1980) *Methods Enzymol. 69*, 392–406.

Vervoort, J., Müller, F., Mayhew, S. G., van den Berg, W. A. M., Moonen, C. T. W., & Bacher, A. (1986) *Biochemistry 25*, 6789–6799.

Vinayaka, C. R., & Rao, V. S. R. (1984) *J. Biomol. Struct. Dyn. 2*, 663–674.

Wagner, G., Neuhaus, D., Wörgötter, E., Vašák, M., Kägi, J. H. R., & Wüthrich, K. (1986) *Eur. J. Biochem. 157*, 275–289.

Westler, W. M., Kainosho, M., Nagao, H., Tomonaga, N., & Markley, J. L. (1988a) *J. Am. Chem. Soc. 110*, 4093–4095.

Williamson, G., & Edmondson, D. E. (1985) *Biochemistry 24*, 7790–7797.

Wüthrich, K. (1986) *NMR of Proteins and Nucleic Acids*, pp 1–292, Wiley, New York.

Wüthrich, K., Wider, G., Wagner, G., & Braun, W. (1982) *J. Mol. Biol. 155*, 311–319.